Journal of Arid Environments 130 (2016) 30–39

Contents lists available at ScienceDirect

Journal of Arid Environments

journal homepage: www.elsevier.com/locate/jaridenv

Fine root distributions of shelterbelt trees and their water sources in an oasis of arid northwestern China

Qingli Xiao [a, b], Mingbin Huang [b, *]

[a] College of Resources and Environment, Northwest A&F University, Yangling 712100, China
[b] State Key Laboratory of Soil Erosion and Dryland Farming on the Loess Plateau, Institute of Soil and Water Conservation, Northwest A&F University, Yangling 712100, China

ARTICLE INFO

Article history:
Received 7 April 2015
Received in revised form
25 October 2015
Accepted 17 March 2016

Keywords:
Sap flow
Irrigation
Water consumption
Water management

ABSTRACT

Shelterbelt trees play an important role in maintaining the sustainability of oases agricultural ecosystems, but the trees require a considerable amount of water for survival. The objectives of this study were to investigate the root distributions, transpiration and water sources of shelterbelt trees (Gansu Poplar; *Populus gansuensis*) in order to improve water management efficiency. Fine root and soil water distributions were investigated along three transects that passed through cropland and an adjacent shelterbelt, while sap flow measurements were conducted on six Gansu Poplar trees. Results showed that roots were mainly distributed within 5 m of both sides of an irrigation channel passing between the first and second tree rows. The maximum distance to which trees extended fine roots horizontally was about 18 m from the shelterbelt. In 2-m soil profiles, fine roots were mainly distributed in the 1.4–2.0 m and 0–0.4 m layers depending on the available water sources. A positive relationship was observed between soil water and fine root mass density. Trees grown near the cropland-shelterbelt border exploited water from cropland irrigation and irrigation channel leakage, greatly enhancing their transpiration. During the growing season of 2013, the mean total transpiration of trees grown farther away from the border (10.75 and 17.45 m) was 216.9 mm, whereas for trees grown nearer to the border (0.85 and 6.30 m) the amounts were 670.1 and 488.7 mm, respectively. If the trees were assumed to absorb the same amount of water from soil, rainfall and groundwater sources, then irrigation water sources provided 67.6% and 55.6% of the water meeting the transpiration requirements of the trees closest to the border. The results have important implications for water management in oasis agricultural areas by limiting the extension of shelterbelt tree roots into adjacent cropland in order to improve irrigation water use efficiency.

1. Introduction

Sandy desertification is one of the important environmental problems confronting the oases agricultural ecosystems in the middle reaches of the Heihe River Basin in northwestern China (Luo et al., 2005). The Heihe River Basin is situated in a desert area and is, therefore, in an inland arid region. The oasis areas support agriculture in an otherwise desert landscape. In order to protect the cropland against damage from sandstorms and dry thermal winds originating in the desert, shelterbelt trees have been planted around and within the oasis areas that cover 84,700 ha. Since the 1980's, the total area covered by these trees has increased to 18,000 ha, according to the Zhangye Water Conservation Bureau of Gansu Province (Zeng et al., 2002; Liu et al., 1997; Chang et al., 2004). The four main species of shelterbelt trees are *Populus gansuensis*, *Populus bolleana*, *Tamarix chinensis*, and *Pinus sylvestris* (Su et al., 2010). Although the shelterbelts effectively protect and improve the environment of the oasis areas, which potentially leads to their sustainability, the shelterbelt trees also require a considerable amount of water in order to survive and grow. Consequently, these trees have increased the demands on the scarce regional water resources. Water consumption in the oases amounts to 86% of the total water resources available from the Heihe River, and irrigation accounts for 96% of the water consumed (Chen et al., 2003). Therefore, it is essential to know the water consumption of, and the water sources used by, the shelterbelt trees in order to facilitate sustainable management of the limited water resources.

The fine roots (diameter <2 mm) are the main means by which

* Corresponding author.
E-mail address: hmingbin@yahoo.com (M. Huang).

http://dx.doi.org/10.1016/j.jaridenv.2016.03.004
0140-1963/

plants absorb water and nutrients, and the spatial distribution of the fine roots in turn directly affects the amounts and distributions of the plant available water and nutrient resources. Previous studies have found that fine root distribution was closely related to rainfall, soil water, soil texture and the water table (Dawson and Pate, 1996; Wilcoxa et al., 2004; Schenk and Jackson, 2005; Zhao et al., 2010; Gang et al., 2012; Imada et al., 2013; Ferrante et al., 2014; Padilla et al., 2015). Typically, most of the fine roots of plants are concentrated in the upper soil layers and the density of the roots notably decreases with increasing soil depth (Schenk and Jackson, 2002; Schenk, 2008). Jackson et al. (1996) reported that the root systems in boreal forests and temperate grasslands were the shallowest, while those in deserts and temperate coniferous forests were the deepest. Drought can result in a redistribution of fine roots to deeper mineral soil horizons in order to access deep soil water resources as well as nutrients (Persson et al., 1995). For example, the maximum root depth under a 12-year-old jujube plantation was 10 m in the absence of irrigation in the semiarid hilly region of the Chinese Loess Plateau (Ma et al., 2013). Tree roots are also able to extend horizontally to exploit water sources; for example, into cropland that was 20 m away from the trees in an agroforestry system in southwestern Australia (Woodall and Ward, 2002). Cheng et al. (2013) reported that the distributions of the fine roots of *Caragana korshinkii* were affected by soil texture; in a sandy soil the fine root density was higher than in a silt loam soil within the upper 0.8-m soil layer, but the opposite was observed in the lower 0.8–2.8 m soil layer.

Tree water consumption can be determined by measuring sap flow. There are many factors influencing tree sap flow, including meteorological factors, soil water and groundwater. The main meteorological factors are solar radiation, air temperature and vapor pressure deficit (VPD). Shen et al. (2015) found that sap flow is positively related to solar radiation, while linear (Gazal et al., 2006) or logarithmic (Shen et al., 2015) functions can both describe relationships between sap flow and VPD under certain conditions due to a complex response of sap flow to VPD. Soil water is a critical factor affecting tree sap flow in arid areas where plants are always growing under water deficit conditions (Zhao and Liu, 2010; Naithani et al., 2012). Groundwater is another factor that influences tree sap flow where there is a relatively shallow water table. Some studies have shown that sap flow increases with decreases in the depth of the water table (Gazal et al., 2006; Ma et al., 2013).

A number of studies have focused on sap flow and its temporal and spatial variations of trees among shelterbelts in the middle reaches of the Heihe River Basin (Chang et al., 2006; Zhao et al., 2007, 2010; Yi et al., 2014). However, little is known about the fine root distributions and the sources of water used by the shelterbelt trees. The shelterbelts around and within the oasis are typical of agroforestry systems. Since the shelterbelts are affected by climate, soil texture, cropland irrigation and shallow groundwater, the root distributions and water consumption of the trees can be more complex in these areas. Therefore, it is important to gain information and to understand the patterns of root distributions and the water sources used by the shelterbelt trees in order to better manage them and to improve water resource use efficiency in the whole Heihe River Basin.

In the presented study, we investigated fine root and soil water distributions along three transects that passed through cropland and an adjacent shelterbelt. We also conducted sap flow measurements for six Gansu Poplars at different distances from the cropland-shelterbelt border. We hypothesized that soil water availability would affect the vertical and horizontal distributions of fine roots. We also hypothesized that the total water consumption of the trees at different distances from the border would be different due to the location-specific limitations of the water sources.

2. Materials and methods

2.1. Site description

The field experiment was conducted between May 1 and October 1 in 2013 at the Linze Ecological Observational and Experimental Station (39°21′N, 100°07′E), which is located in a desert-oasis ecotone in the middle reach of the Heihe River Basin of Northwest China (Fig. 1a). This area has a continental arid temperate climate with a mean annual precipitation of 116.8 mm (1965–2000), about 90% of which falls during the rainy season between June and September. The annual mean air temperature is about 7.6 °C, and the mean maximum and minimum temperatures, which occur in August and December, are 39.1 °C and −27.8 °C, respectively. The mean annual open water evaporation is about 2365 mm (Chang et al., 2006). The mean frost-free period is 165 days, and the relative humidity ranges from 7.3% to 80.9% (Ji et al., 2007). During the study period, the mean monthly temperature was 20.4 °C and the mean precipitation was 50.5 mm.

2.2. Experimental design and measurements

An 80 m × 16 m experimental plot was selected to pass through spring wheat cropland (for 22 m of its length), a shelterbelt with 9 rows of trees (for 36 m), and maize cropland (for 22 m). In this study, only the spring wheat cropland and half of the shelterbelt (i.e., 4 tree rows) adjacent to the spring wheat field were investigated. The shelterbelt trees were Gansu Poplars (*P. gansuensis*) that were planted in 1980 with row spacing ranging from 4.45 to 6.7 m. The growing season of Gansu Poplars was from May 1 to October 1 in 2013. An irrigation channel with a depth of 0.5 m and a mean width of 0.65 m had been constructed between the first and second rows (Fig. 1b), from which sub-irrigation channels transferred water to the spring wheat crop, while the maize crop was irrigated only through another main channel located outside of the study area. During the growing seasons of spring wheat (March 6 to July 10), the crops were irrigated every 7–14 days with approximately 100 mm of water on each occasion; a further irrigation (100 mm) was applied at the beginning of the winter season (November 5) after sowing the spring wheat. During the growing season of the spring wheat, the bed and sides of the irrigation channel were sealed with a thin plastic sheet to prevent water leakage for further studying the effect of irrigation channel leakage to tree transpiration. The plastic was removed after July 27. From July 27 to September 30, water was permitted to leak from the irrigation channel for a total duration of 241 h; no irrigation was conducted from September 30 to November 5. During the study period from May 1 to September 30, 2013, ten irrigations supplied a total of 960.8 mm of water to the spring wheat crop, while the amount of rainfall was 105.6 mm (Fig. 2). With regard to the crops, the irrigation schedule was designed to ensure that the crops did not suffer water stress. Actually, excessive irrigation was used to ensure excess salts were prevented from accumulating in the soil profile.

2.2.1. Soil water measurements

Three 44.56-m long transects, 4 m apart, were laid out through the spring wheat cropland (18.66 m) and the first four rows of the adjacent shelterbelt trees (25.9 m). Eight polycarbonate Trime Domain Reflectometry (Trime-TDR) access tubes (4 cm in diameter and 300 cm long) were installed in the soil along each transect to facilitate multiple determinations of water content over time and space under the cropland and shelterbelt (Fig. 1b). The distance

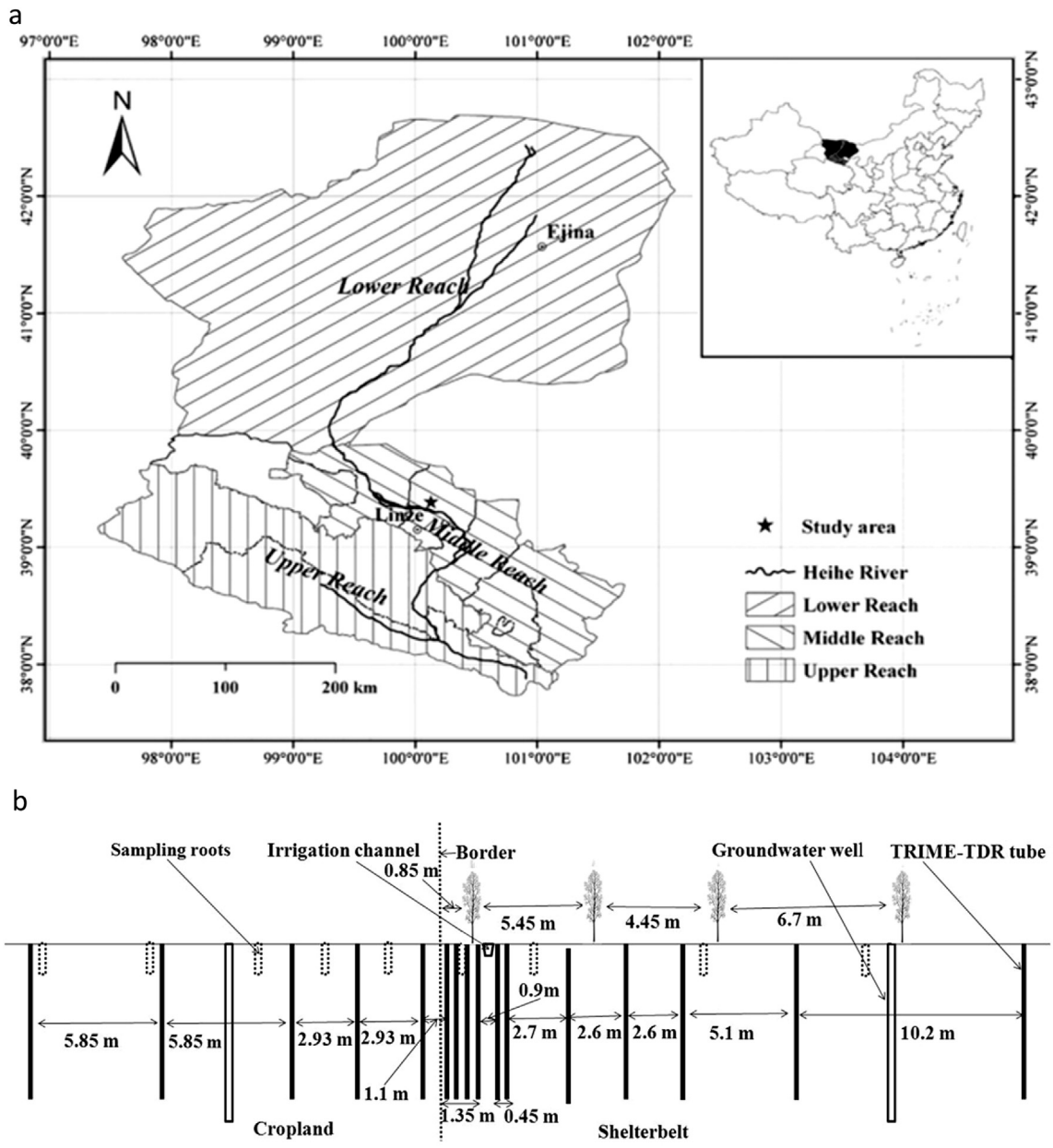

Fig. 1. (a) Location of the study site in the Heihe River Basin, China, and (b) the layout of a cropland-shelterbelt transect at the study site.

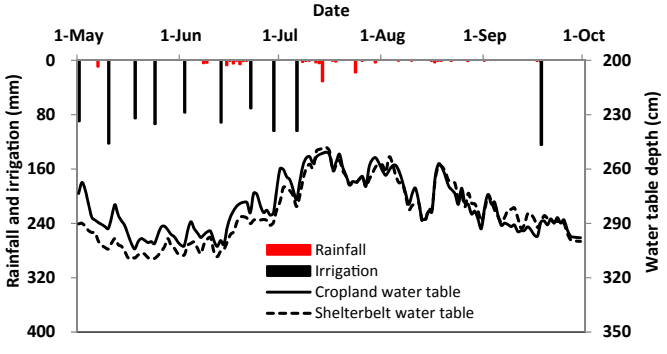

Fig. 2. Rainfall, cropland irrigation and water table depth during the study period in 2013.

between adjacent tubes ranged from 0.45 to 5.85 m. At each tube location, the volumetric soil water content was measured by the Trime-TDR (TRIME-TDR-PICO-IPH-T3, Imko, Germany) at 10-cm depth increments between the depths of 10 and 280 cm. The measurements were made every 5 days during the study period. Additional measurements were conducted before and after irrigation as well as after rainfall events. The Trime-TDR was calibrated in the field against measurements made by the gravimetric method under both dry and wet conditions.

2.2.2. Sap flux and transpiration measurements

Nine shelterbelt trees in four rows nearest to the cropland were chosen for sap flow measurements. Three trees were in each of the first two rows, while two trees were in the third row and one was in the fourth row. All trees were located in the experimental plot and had similar diameters at breast height (DBH, Table 1). The distances of the four rows from the cropland-shelterbelt border were 0.85,

Table 1
Biometric and physiological parameters of six trees used for sap flow measurements at different distances from the edge of the shelterbelt.

No. of tree row	Distance from cropland-shelterbelt border (m)	Diameter at breast height (cm)	Height (m)	Sapwood radius (cm)	Sapwood area (cm^2)	Canopy projected area (m^2)
1	0.85	29.62	21.47	6.81	487.65	29.60
1	0.85	30.24	22.51	4.81	342.50	26.36
2	6.30	32.48	24.32	6.24	514.34	25.58
2	6.30	29.05	21.39	4.57	318.35	25.20
3	10.75	28.66	20.85	3.33	264.96	22.63
4	17.45	31.85	20.42	3.22	289.73	28.97

6.30, 10.75 and 17.45 m, respectively (Fig. 1b). The sap flux was measured using the thermal dissipation method by constant heat flow gauges (Du et al., 2011). A Granier-type thermal dissipation sensor (TDP30, Dynamax. Inc., Houston, Texas, USA) was inserted into each of the sampled trees and remained in place during the entire growing season. Each sensor consisted of a pair of probes, 30-mm long and 1.2-mm in diameter. Each probe contained a copper-sontantan thermocouple. Two sensors were inserted along a horizontal radius of the tree trunk at breast height, one vertically above the other. The upper probe, which also had a heat source, was supplied with 0.2 W of constant power, while the lower probe was used as an unheated reference. Aluminum foil covered the probes and trunk in order to protect them from the effects of direct solar radiation and to reduce the effects of ambient temperature fluctuations.

The temperature difference between the upper heated probe and the lower unheated reference probe was measured and converted to sap flow density (SF_d) using an empirical calibration equation determined by Granier (1987).

$$SF_d = 0.0119\left(\frac{\Delta T_m - \Delta T}{\Delta T}\right)^{1.231} \quad (1)$$

where SF_d is the sap flow density (g cm^{-2} s^{-1}); ΔT is the temperature difference between the two probes (°C); and ΔT_m is the maximum temperature difference under conditions of zero sap flow, which are assumed to occur at 2 a.m. in the night (°C). The assumption made about the occurrence of zero sap flow was considered reasonable since, during the night, VPDs are typically low and the temperature gradients detected by the sensors attain equilibrium during most nights (Dierick and Holscher, 2009). Temperature differences were monitored at 10-s intervals and were logged every 30-mins as the mean value of the data collected over that period by a CR1000 data logger (Campbell Scientific Inc., Logan, UT, USA). The daily sap flux (SF) of individual trees was calculated using the determined values for the SF_d and the sapwood area in the following equation:

$$SF = \frac{24 \times SF_d \times A_s \times 3600}{1000} \quad (2)$$

where SF is the sap flow (kg d^{-1} $tree^{-1}$) of an individual tree and A_s is its sapwood area (cm^2), which was calculated from an empirical equation developed by Chang et al. (2006) that related measured DBH and to sapwood area at the same site.

Daily transpiration (T_r) of an individual tree was calculated using the following equation:

$$T_r = \frac{SF}{S} \quad (3)$$

where T_r is the daily transpiration (mm d^{-1}) of an individual tree and S is the canopy projected area (m^2).

During the entire growing season, only six of the sensors worked correctly; hence only the biometric parameters of the six sampled trees for which successful sap flow measurements were made are shown in Table 1.

2.2.3. Fine root measurements

The fine root distributions of the shelterbelt trees were measured along one of the outer transects using the trench-profile method (Böhm, 1979). Nine soil pits (2 m deep by 4 m long by 1 m wide) were dug in September to take samples at intervals along the length of the cropland – shelterbelt tree transect (Fig. 1b). Four pits were located among the shelterbelt trees at distances from the border between the cropland and shelterbelt of 1, 5, 10, and 15 m, while the other five were located in the wheat field at distances from the border of −1.4, −4, −7.5, −13, and −18 m. All of the soil pits were dug with their lengths parallel to the border. At each of the nine sampled locations along the transect, only one large soil pit was excavated from which three sets of profile fine root data were obtained, rather than excavating three separate smaller pits. Excavation of the three smaller pits would have necessitated excavation of the surrounding area as well in order to gain access to the pits for sampling. Therefore, a smaller total excavation area was achieved by using the one large pit. This decreased the workload but, more importantly, it reduced the destruction within the experimental plot, which was especially important within the uncultivated shelterbelt. Replication was then achieved by sampling at three separate locations within 0.5 m × 0.2 m grids placed at intervals along the length of the large pit. During excavation, at each depth interval, the grids were placed at the base of the pit. One grid was placed at each end of the soil pit and one grid was in the middle of the pit. The separation distance for any two neighboring grids was 1.25 m. Tree roots were collected selectively from each grid at each of the three locations at 0.1-m depth increments to a total depth of 2 m. This task required 3 people working for 9 days to excavate and sample all of the pits at the nine locations. The roots collected from each grid and depth interval were washed over a sieve under running tap water to remove the soil. The washed fine roots (<2 mm diameter) were collected from the sieve and the total root dry mass was then determined by initially drying in an oven for 30 min at 105 °C and then at 80 °C until constant mass was attained. The fine root mass density (dry mass of root per unit soil volume, FRMD) was determined for each soil grid sample.

2.2.4. Measurements of soil properties

Undisturbed soil samples were collected from the soil profile walls exposed when digging the pits for the fine root sampling. From each soil pit, three samples were collected at each 0.2-m depth increment to a depth of 2 m using stainless steel cutting rings that were 0.05 m long and 0.05 m in diameter. The same method was used as the fine root sampling collection. Twelve replications were collected at each depth under the shelterbelt, i.e., three per depth per pit for the four pits under among the trees, while fifteen replications were collected from the wheat field, i.e., three per depth per pit for the five pits in the cropland. These

Table 2
Soil physical properties under the cropland and shelterbelt.

Land use type	Soil layer (m)	Soil texture			Bulk density (g cm^{-3})	Field capacity (cm^3 cm^{-3})	Soil texture classification
		Clay (%)	Silt (%)	Sand (%)			
Cropland	0–0.4	10.35 ± 1.43	15.28 ± 1.19	74.37 ± 3.53	1.43 ± 0.027	0.101 ± 0.007	Sandy loam
	0.4–1.4	8.26 ± 1.21	10.18 ± 1.26	81.56 ± 5.49	1.55 ± 0.032	0.092 ± 0.004	Loamy sand
	1.4–2.0	39.24 ± 3.19	41.48 ± 3.57	19.28 ± 1.35	1.52 ± 0.014	0.194 ± 0.008	Silty clay loam
Shelterbelt	0–0.4	15.73 ± 1.28	18.42 ± 1.74	65.85 ± 3.64	1.39 ± 0.018	0.094 ± 0.002	Sandy loam
	0.4–1.4	16.49 ± 1.63	15.54 ± 1.42	67.97 ± 3.56	1.60 ± 0.021	0.083 ± 0.002	Sandy loam
	1.4–2.0	44.39 ± 3.81	49.33 ± 3.26	6.28 ± 0.72	1.49 ± 0.022	0.201 ± 0.007	Silty clay

Table 3
Water sources used for transpiration by shelterbelt trees at different distances from adjacent cropland.

No. of tree row	Distance of trees from the cropland	Mean transpiration rate	Mean total transpiration	Water source			
				Rainfall, groundwater and soil water	Ratio	Cropland irrigation and irrigation channel leakage	Ratio
	(m)	(mm d^{-1})	(mm)	(mm)	(%)	(mm)	(%)
1	0.85	4.4 ± 2.0	670.1	216.9	32.4	453.2	67.6
2	6.30	3.2 ± 1.5	488.7	216.9	44.4	271.8	55.6
3	10.75	1.3 ± 0.6	206.1	216.9	100.0	0.0	0.0
4	17.45	1.4 ± 0.6	227.7	216.9	100.0	0.0	0.0

Mean transpiration rates given as the mean value ± the standard deviation.

samples were used for: (1) producing soil water characteristic curves using the centrifugation method (Townend et al., 2001) (Hitachi CR21G centrifuge; 20 °C) at suctions of 0.001, 0.005, 0.01, 0.02, 0.04, 0.06, 0.08, 0.1, 0.2, 0.4, 0.6, 0.8, 1.0, and 1.5 MPa, from which field capacity and other important parameters could be determined; (2) determining the soil particle-size distribution by laser diffraction (Laser Scattering Particle Size Distribution Analyzer Model LA-950, Horiba Instruments Inc., 2008) for 93 particle diameters between 3.0 mm and 1.1e-05 mm; and (3) calculating soil bulk density based on the volume of the soil core and its mass after oven-drying at 105 °C to constant mass (ASTMC29/C29M-09, 2003). Pertinent soil physical properties of different soil layers under the cropland and the shelterbelt are shown in Table 2. Table 2 divides the soil profile into three main layers that differed notably.

2.2.5. Groundwater level measurements

One groundwater level monitoring well was established in both the cropland and the shelterbelt areas (Fig. 1b). The depth to the water table was automatically recorded every 20 min by a water-level logger (Hobo U20-001-04, Onset Computer Corporation, Bourne, USA).

2.2.6. Meteorological data

Relative humidity, air temperature, solar radiation, wind speed, atmospheric pressure, and precipitation were measured by an AG1000 automatic weather station (Onset Computer Corporation, Pocasset, MA, USA) at a distance of about 500-m from the study area. The meteorological data were recorded every 5 min by a CR1000 data logger (Campbell Scientific Inc., Logan, UT), which then calculated and stored the mean values of the data collected in each 30-min interval, while precipitation and wind data were stored in each 10-min interval. Reference crop evapotranspiration (ET_0, mm) was calculated using the FAO56 Penman–Monteith equation (Allen et al., 1998).

2.3. Data analyses

The variogram procedure for Geostatistic analysis in SAS (SAS Institute, 2008) was used with kriging to produce the maps of temporal and spatial variations in soil water content under cropland and an adjacent shelterbelt. The relationship between the mean soil water contents and relative fine root mass densities in different soil layers was examined using the REG procedure in SAS.

3. Results

3.1. Temporal and spatial variations in soil water content

The temporal and spatial variations in the soil water content of different soil layers under the cropland and shelterbelt are shown in Fig. 3. The time series of the soil water contents between two land use types showed notable differences because of the differences in precipitation, irrigation, irrigation channel leakage, and groundwater amounts and their roles that affected each land use type. During the growing season of the spring wheat, from May 1 to July 10, there were nine distinct soil water content pulses in the upper soil layer (0–0.4 m) of the cropland that coincided with cropland irrigation events (Figs. 3a and 2). No such pulse was observed in the same soil layer in the shelterbelt because there was no irrigation. Furthermore, such well-defined pulses ceased in this soil layer between mid-July and mid-September when irrigation did not occur. As shown in Fig. 3b and 3c, soil water content pulses in the 0.4–1.4 m and 1.4–2.0 m layers of cropland became less evident with increasing soil depth. Irrigation events resulted in the water table depths under the cropland and the shelterbelt ranging from 3.1 to 2.6 m during this period (Fig. 2). The highest water table of 2.6 m was considerably below the middle and lowest soil layers and was even below the lowest layer. The pulse would become weaker and more diffuse in lower soil layers since the soil water content in these layers was affected by the combination of irrigation and precipitation. The main effect of water infiltration was observed in the upper layer, where wetting and drying processes were more evident due to ET and irrigation and/or rainfall.

During the period from July 10 to October 1, 2013, seven soil water content pulses appeared in the soil layers near the border between the cropland and the shelterbelt due to irrigation channel leakage, which was permitted to occur at this time. As shown in Fig. 3, soil water content pulses were stronger with increasing soil layer depth. This occurred because irrigation channel leakage would be faster at greater depths along the channel due to the

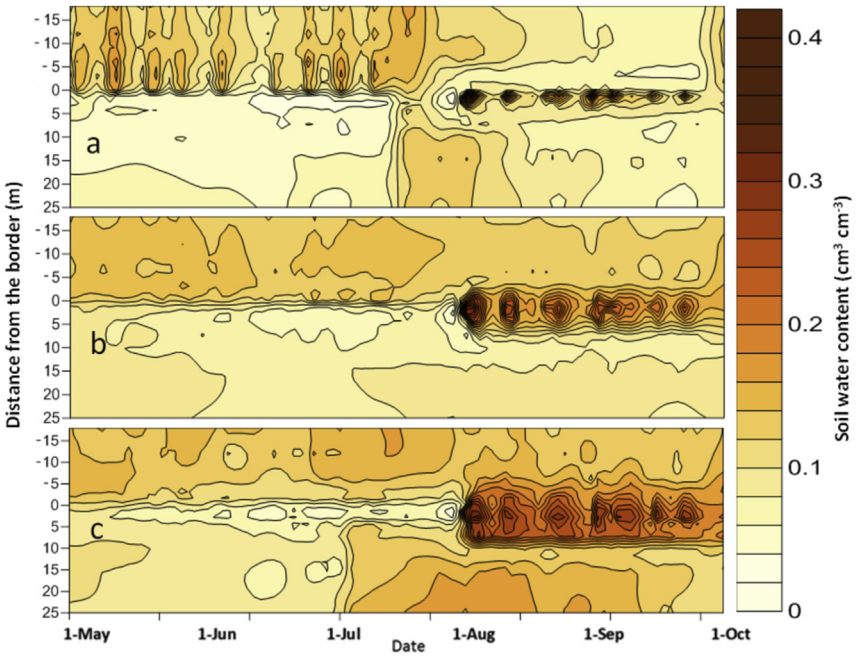

Fig. 3. Temporal and spatial variations in soil water content under cropland and an adjacent shelterbelt divided by a border during the study period in different soil layers: (a) 0–0.4 m, (b) 0.4–1.4 m, and (c) 1.4–2.0 m. Note: distances from the border are negative for the cropland and positive for the shelterbelt.

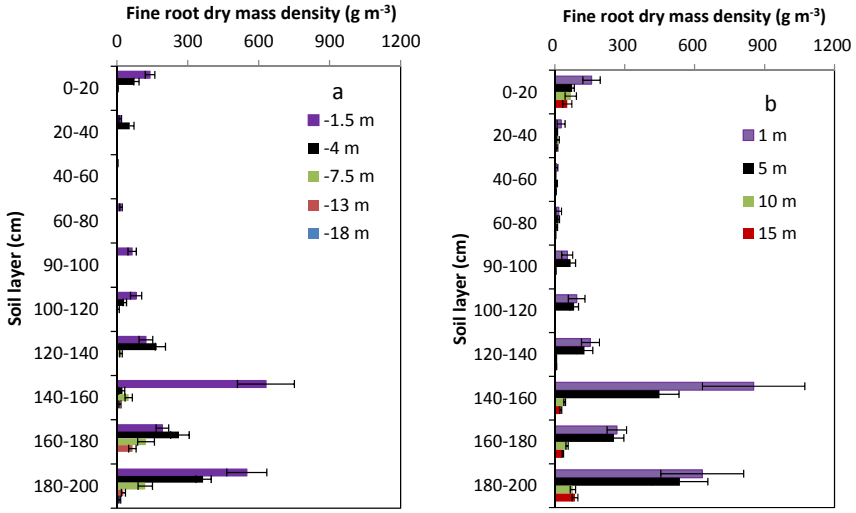

Fig. 4. Vertical distributions of fine root dry mass density under (a) cropland and (b) shelterbelt trees at different distances from the cropland-shelterbelt border.

increased water head. Consequently, the adjacent soil profiles would wet at a faster rate and to a greater extent in deeper layers than the shallower layers. With increasing distance from the irrigation channel, soil water content pulses became weaker. Irrigation channel leakage affected soil water contents to a distance of about 1.4 m away from irrigation channel in the upper layer (0–0.4 m), to about 2.5 m in the middle layer (0.4–1.4 m), and to about 5 m away in the lower layer (1.4–2 m). During the entire study period, the soil water content tended to have higher values in the lower layer than in the upper and middle layers under both land use types.

3.2. Fine root distribution of shelterbelt trees

Most of the fine roots of the shelterbelt trees were present in the 1–2 m soil layer and fine roots increased significantly ($P < 0.01$) with increasing soil depth (Fig. 4). However, the vertical distributions of the FRMD were obviously different between the cropland and the shelterbelt areas (Fig. 4). Under the cropland, the FRMD values in the lower soil layer (1.4–2 m) represented 75.6% and 66.6% of the total fine roots in the profiles at distances of −1.5 and −4 m from the border, respectively. In the upper soil layer (0–0.4 m) at the same distances, FRMD was only 8.5% and 13.1%, respectively. When the distances into the cropland were −7.5, −13 and −18 m from the border, the FRMD values in the lower soil layer were 91.6%, 100% and 100% of the total fine roots in the profile, respectively (Fig. 4a). Very few fine roots, if any, were found in the upper soil layer at these distances. In the shelterbelt near to the irrigation channel, the FRMD values in the lower soil layer were 77.6% and 76.5% of the total fine roots in the profiles at distances of 1 and 5 m from the border, respectively, while the FRMD values in

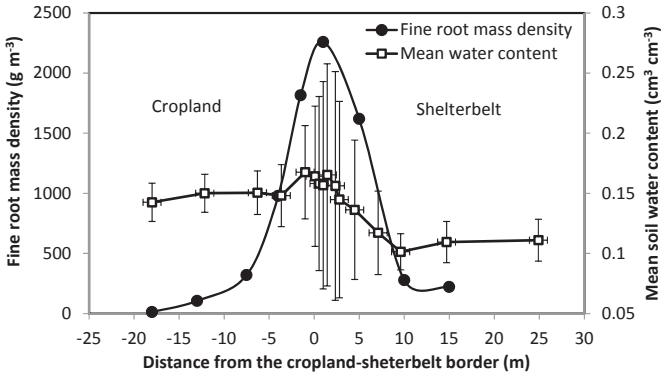

Fig. 5. The horizontal distribution of fine root mass density in the cropland-shelterbelt ecotone.

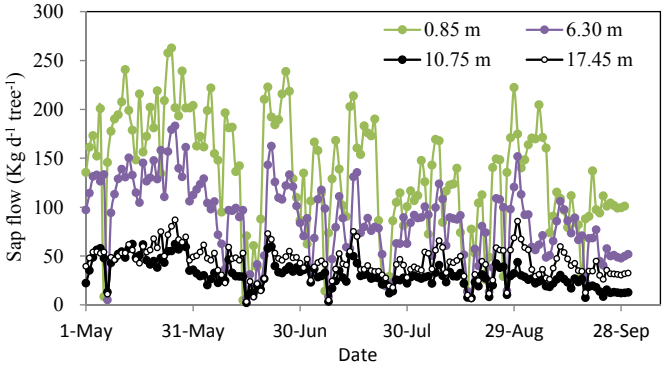

Fig. 6. Daily variations of sap flow of trees at different distances from the cropland-shelterbelt border during the growing season of 2013.

the upper soil layer were only 8.2% and 5.1%, respectively. When the distances were extended to 10 and 15 m from the border into the shelterbelt and away from the irrigation channel, the FRMD values in the lower soil layer were reduced to 61.5% and 66.0% of the total fine roots, respectively, while those for the upper soil layer were increased to 29.3% and 28.2%, respectively (Fig. 4b).

Fine roots extended horizontally from the trees to a maximum distance of approximately 18 m into the cropland (Fig. 5). The fine roots were mainly distributed within 5 m of both sides of an irrigation channel that passed between the first and second tree rows, in order to exploit the leakage for water uptake.

3.3. Variation of daily sap flow

The daily sap flow for trees at different distances from the border was obviously different (Fig. 6). Compared with the trees farther away from the border, the trees nearer the border and the irrigation channel had higher sap flows and exhibited a greater degree of variation over time. During the study period, the mean daily sap flow (± the standard deviation) was 135.5 ± 58.3, 86.3 ± 39.1, 30.4 ± 13.7 and 43.0 ± 16.3 kg d^{-1} $tree^{-1}$ for the trees sampled at distances of 0.85, 6.30, 10.75 and 17.45 m from the border, respectively; the total amount of sap flow was 20737.4, 13289.6, 4663.5 and 6596.2 kg, respectively. Taking into account the effects of cropland irrigation and irrigation channel leakage, the variation in daily sap flow could be divided into two periods: (1) the period of cropland irrigation from May 1 to July 26; and (2) the period of irrigation channel leakage from July 27 to September 30. During the first period, the daily sap flow of the trees nearer the

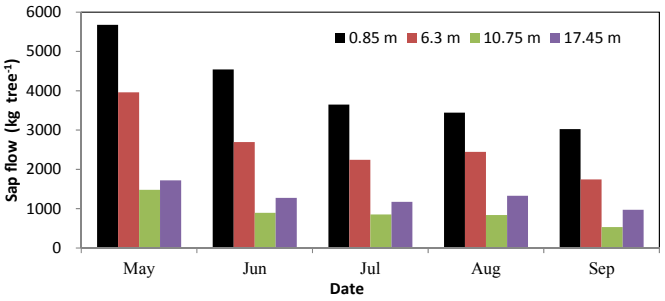

Fig. 7. Monthly variations of sap flow of trees at different distances from the cropland-shelterbelt border during the study period in 2013.

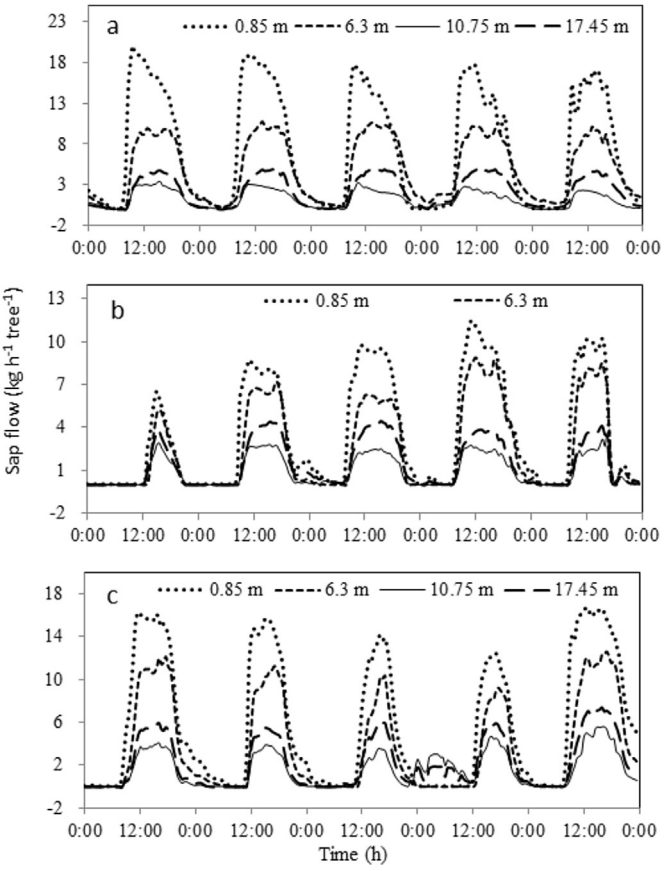

Fig. 8. The responses of diurnal sap flow of trees at different distances from the cropland-shelterbelt border to (a) cropland irrigation, (b) irrigation channel leakage, and (c) rainfall.

border gradually decreased, while the daily sap flow of the trees farther away from the border remained almost constant. During the second period, the daily sap flow of the trees nearer the border increased to a maximum value on August 30, before rapidly decreasing. In contrast, the daily sap flow of the trees farther away from the border remained almost constant. The monthly cumulative sap flow of trees at different distances from the border also presented obvious differences (Fig. 7). During the growing season of the trees, the monthly cumulative sap flow for the trees nearer to the border decreased, while the monthly cumulative sap flow for the trees farther away from the border did not exhibit notable decreases.

3.4. Responses of sap flow to cropland irrigation, rainfall and irrigation channel leakage

Responses of sap flow to cropland irrigation, rainfall, and irrigation channel leakage were different at different distances from the border (Fig. 8). The sap flow of the two trees nearer to the border started between 08:00 and 09:00 h on the day before a cropland irrigation event, and began about 1 h earlier after the irrigation had occurred. However, the time at which the sap flow began (between 09:00 and 09:30 h) in the two trees farther away from the border was not affected by cropland irrigation events (Fig. 8a).

During the period of irrigation channel leakage, the sap flow of the two trees nearer to the border increased sharply between 08:00 and 08:30 h, and reached a maximum value between 10:30 and 13:00 h. The sap flow of these two trees was also greater at night than that of the two trees farther away from the border. The sap flow of the two trees farther away from the border was not affected by the occurrence or lack of irrigation channel leakage (Fig. 8b).

The mean sap flow of the trees farther away from the border was 39.18 kg d^{-1} $tree^{-1}$ in the days before rainfall events occurred. After rainfall events, the sap flow in these trees was 1.49 times higher, and the sap flow at night was also higher. However, the mean sap flow of the trees nearer to the border was not obviously affected by the occurrence of rainfall events (Fig. 8c).

3.5. Water sources used in shelterbelt tree transpiration

The transpiration rate and total water consumption of the trees at different distances from the border were different. During the growing season, the mean transpiration rate of the trees at distances of 0.85, 6.30, 10.75 and 17.45 m from the border was 4.4 ± 2.0, 3.2 ± 1.5, 1.3 ± 0.6 and 1.4 ± 0.6 mm d^{-1} (Table 3), respectively. The mean cumulative transpiration of the two trees at 10.75 and 17.45 m from the border was 216.9 mm. Due to the longer distance from the cropland and irrigation channel, almost all of the water used for transpiration could be assumed to come from rainfall, soil water, and groundwater. The mean total transpiration of the two trees at 0.85 and 6.30 m from the border was 670.1 and 488.7 mm, respectively. An assumption could be made that the same amount of water was used by the trees nearer the border for transpiration from rainfall, soil water, and groundwater as by the other two trees, i.e., 216.9 mm. Accordingly, the remaining transpiration of the nearer trees would come from cropland irrigation and irrigation channel leakage for the trees at 0.85 and 6.30 m, representing 67.6% and 55.6% of the total transpiration (Table 3), respectively.

4. Discussion

4.1. Fine root distributions of shelterbelt trees

Fine root distribution is largely influenced by soil resource availability (Bennett et al., 2002; Hodge, 2004; Tanasescu and Paltineanu, 2004; Zhou and Shangguan, 2007; Cheng et al., 2013; Imada et al., 2015). Fine roots concentrate near the soil surface and exponentially decrease with increasing soil depth in most ecosystems (Schenk, 2008). This distribution pattern of fine roots suggests that it results from a dependence on rainfall and/or irrigation as the main water sources. However, under the shelterbelt in our study area the fine roots of the shelterbelt trees were mainly concentrated in the upper and lower soil layers; 17.7% of the mean total fine root mass was found in the upper 0.4-m layer, whereas 70.4% were located at the depths between 1.4 and 2.0 m. In the cropland, a greater proportion (86.6%) of the mean total fine tree root mass was concentrated in the lower soil layer, and only 4.5% of the fine tree roots were found in the upper layer. This might be due to the destruction of the tree root system caused by the cultivation of the upper 20-cm soil layer every year. The low amounts of fine roots at depths between 0.4 and 1.4 m is likely due to the relatively low soil water contents (Fig. 3).

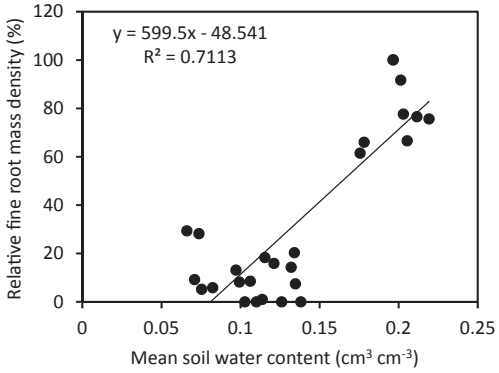

Fig. 9. The relationship between the mean soil water content during the growing season of Gansu Poplars and relative fine root mass density to the total fine roots in different soil layers.

In this study, the FRMD was strongly and positively correlated with the mean water content of the soil (Fig. 9), although other soil factors may have influenced the fine root distribution. This observation was also supported by previous findings. A linear reduction in fine root growth with decreasing soil water at less than field capacity has been reported for *Populus alba* cuttings (Imada et al., 2008). A weak but positive relationship between fine root biomass and soil water has also been reported for *Tamarix ramosissima* (Imada et al., 2013).

It is notable that the fine root distribution in the soil profile in the shelterbelt varied with the distance from the border (Fig. 4b). The FRMD values in the upper soil layer increased with increasing distance from the border. Close to the border, at distances of 1 and 5 m, the FRMD values in the upper soil layer were only 8.2% and 5.1%, respectively. Farther from the border, at distances of 10 and 15 m, the FRMD values in the upper soil layer were increased to 29.3% and 28.2% of the total fine roots, respectively. The mean soil water contents during the growing season of Gansu Poplars were 0.099, 0.075, 0.066, and 0.074 cm^3 cm^{-3} in the upper soil layer for these four locations, respectively. A positive relationship between fine root mass and soil water content was not found for the upper soil layer in the shelterbelt. The reason might be due to the hydraulic lift or hydraulic redistribution characteristics of the roots whereby a tree can take up water from where it is relatively more abundant and exude it through lateral roots where there is a water deficit (Kizito et al., 2007). In the study area, roots located at distances of 10 and 15 m from the border could not absorb water from cropland irrigation and irrigation channel leakage. Therefore, almost all of the water used for transpiration came from rainfall, soil water, and groundwater. During the dry period, the shelterbelt trees could suck up water from the groundwater and replenish the dryer layers by hydraulic lift of the roots (Caldwell et al., 1998; Hao et al., 2013). Caldwell et al. (1998) reported that the process of hydraulic lift by roots can enhance fine root activity in upper soil layers as well as the redistribution of nutrients from the depth where the water source is to other soil layers (McCulley et al., 2004). Armas et al. (2012) found that hydraulic lift of roots played a positive role in organic matter decomposition and N uptake by plants. Thus, the water in the upper soil layers that was probably driven by the root systems may also enable the plant to capture N

from the soil where N concentrations were higher (Imada et al., 2013). The N concentration profiles in the shelterbelt were not investigated in this study but future studies should address the effect of available nutrients on fine root distributions of the shelterbelt trees in arid inland river basins.

This study showed that the fine roots of the shelterbelt trees were mainly distributed along both sides of, and within 5 m of, the irrigation channel (Fig. 5). This result was in agreement with other studies on shelterbelt trees in arid regions (Woodall and Ward, 2002; Shen et al., 2014). The findings of this study indicate that large amounts of available water from both cropland irrigation and irrigation channel leakage promoted root growth near the border between the shelterbelt and the irrigated cropland. The shallow groundwater depth caused fine roots to be mainly distributed in the 1.4–2 m soil layer where the water source was abundant under both the cropland and the shelterbelt. In contrast, the limited rainfall and restricted hydraulic lift of roots resulted in a smaller proportion of fine roots being distributed in the upper 0.4-m soil layer of the shelterbelt.

4.2. Water sources used in shelterbelt tree transpiration

In this study, the mean transpiration rates of the trees in the shelterbelt that were nearer to the border (0.85 and 6.30 m) were 4.4 and 3.2 mm d^{-1}. Considerably lower transpiration rates (1.3 and 1.4 mm d^{-1}) were measured for the trees farther away from the border (10.75 and 17.45 m). Under irrigation conditions, the mean transpiration rate of trees in the study area ranged from 1.7 to 5.6 mm d^{-1}, depending on the diameter at breast height and other factors (Chang et al., 2006). Therefore, the trees were likely to be affected by water stress to a higher degree when they were farther from the border than when they nearer to it during the summer growing season. The trees nearer to the border were not dependent on rainwater and groundwater alone, but could also take up large amounts of irrigation water from either the irrigated cropland soils or the irrigation channel leakage. The fine root distributions of shelterbelt trees measured in the cropland soil provided strong evidence that the trees were exploiting the water and other resources of the cropland soil. In contrast, the two trees farther away from the border depended almost entirely on rainwater and groundwater, which was less likely to be sufficient to meet their transpiration requirements.

In this study, the contributions of groundwater, soil water and rainwater uptake to tree transpiration were not fully accounted for. Shen et al. (2015) calculated the amount of groundwater and soil water uptake for tree transpiration using the soil water balance approach on the basis that trees used soil water preferentially and, subsequently, groundwater when soil water storage was insufficient to meet transpiration requirements. Their results indicated that the groundwater uptake accounted for 19% of tree transpiration during the growing season of 2013 in the same area as our study. Pinto et al. (2013) estimated the yearly groundwater contribution to the transpiration of *Quercus suber* to be 30.3%, whereas groundwater uptake became dominant in the dry summer to account for 73.2% of the transpiration. The contribution of groundwater to tree transpiration varied with rainfall conditions. The results reported by Vincke and Thiry (2008) indicated that the contribution of groundwater to a Scots pine stand (*P. sylvestris*) transpiration during May–November was 61%, whereas it was as much as 98.5% during the drought period in June. Cramer et al. (1999) reported that groundwater provided over 70% of the water source for *Casuarina glauca* transpiration during their study period, whereas the contribution of groundwater to transpiration was less than 40% during periods with high rainfall.

In our study, the trees nearer the sources of irrigation water exhibited large variations in sap flow while the trees farther away from those water sources did not. The variability of the trees that could use the irrigation water clearly reflected the irrigation cycle whereas the trees to which irrigation water was not accessible relied upon relatively constant supply of other water sources. The water consumption was almost doubled when the trees were near the sources of irrigation water than when they were farther away from them. This indicates that the un-irrigated trees are surviving by root water uptake from the soil, rainfall, and groundwater, but the irrigated ones are thriving by using water that would better be reserved for crops. The results have important implications for water management in the study area. A management plan to largely limit the access of these trees to the irrigation water in the cropland should be recommended for improving irrigation water use efficiency. For example, regular deep cultivation of the cropland soil adjacent to the shelterbelt might be adopted in order to destroy the tree roots that extended into the cropland.

The irrigation channel leakage also provided a part of the water used for transpiration by the trees nearer to the border. In order to improve water use efficiency, the leakage from the irrigation channel could be prevented by improving the construction of the irrigation channel. However, allowing the channel to leak has previously been considered to facilitate the survival of the trees on the exposed edge of the shelterbelt. Preventing channel leakage could be detrimental to the shelterbelt and competition among the trees for water might put pressure on the groundwater resource. Possibly, the shelterbelt could be irrigated under controlled conditions in order to meet the basic water requirements of all of its trees to ensure their survival. This might improve the water use efficiency as well as the health of the shelterbelt. Further research should be conducted to examine this issue.

In this study, the contributions of groundwater, soil water and rainfall to tree transpiration were not partitioned, but all trees were assumed to absorb the same amount of water from soil, rainfall and groundwater sources. This assumption could result in an error when partitioning the contributions of the different water sources. Numerical models and isotope tracing should be considered for further study that quantifies the contributions of different water sources.

5. Conclusions

This study investigated the fine root distributions and transpiration rates of Gansu Poplar shelterbelt trees in an agricultural area of an oasis in the Heihe River Basin and identified sources of water exploited by the trees. The fine root distributions were affected by rainfall, groundwater, adjacent cropland irrigation and irrigation channel leakage as well as by soil water. The maximum depth and the farthest horizontal distance of the fine roots were approximately 2 and 18 m, respectively. Fine roots were concentrated along both sides of the irrigation channel to a distance of 5 m. Within the soils under the adjacent cropland and under the shelterbelt, the fine roots were concentrated in the 1.4–2.0 m soil layer and in the upper 0.4 m layer, respectively. In addition, there were some concentrations of fine roots in the 1.4–2.0 m layer of clayier soil within the shelterbelt.

During the growing season of the trees, the mean total transpiration of the trees growing 10.75 and 17.45 m away from the cropland-shelterbelt border was 216.9 mm, and the water that met this demand was almost entirely provided by rainwater, soil water and groundwater uptake. In contrast, the total transpiration amounts of the two trees within 0.85 and 6.30 m of the border were 670.1 and 488.3 mm, respectively, of which 67.6% and 55.4% was estimated to be provided by water from cropland irrigation and irrigation channel leakage, while the remainder was provided by

rainfall, soil water and groundwater uptake.

These results have important implications for water management in the study area. The irrigation water use efficiency could be improved by limiting the access of the shelterbelt tree roots to irrigation water.

Acknowledgments

This research was financially supported by the National Natural Science Foundation of China (No. 41571213). We would like to thank the Linze Inland River Basin Comprehensive Research Station, Chinese Ecosystem Research Network.

References

Allen, R.G., Pereira, L.S., Raes, D., Smith, M., 1998. Crop Evapotranspiration (Guidelines for Computing Crop Water Requirements). FAO Irrigation and drainage paper 56, Rome, Italy.

Armas, C., Kim, J.H., Bleby, T.M., Jackson, R.B., 2012. The effect of hydraulic lift on organic matter decomposition, soil nitrogen cycling, and nitrogen acquisition by a grass species. Oecologia 168, 11–22.

ASTMC29/C29M-09, 2003. Standard Test Method for Bulk Density (Unit Weight) and Voids in Aggregate. In: Annual Book of ASTM Standards. Section 4: Soil and Rock, vol. 04.08. American Society for Testing Materials, West Conshohocken, PA.

Bennett, J.N., Andrew, B., Prescott, C.E., 2002. Vertical fine root distributions of western redcedar, western hemlock, and salal in old-growth cedar-hemlock forests on northern Vancouver Island. Can. J. For. Res. 32, 1208–1216.

Böhm, W., 1979. Methods of Studying Root Systems. Springer, Berlin.

Caldwell, M.M., Dawson, T.E., Richards, J.H., 1998. Hydraulic lift: consequences of water efflux from the roots of plants. Oecologia 113, 151–161.

Chang, X.X., Zhao, W.Z., He, Z.B., 2004. Radial pattern of sap flow and response to microclimate and soil moisture in Qinghai spruce (Picea crassifolia) in the upper Heihe River Basin of arid northwestern China. Agric. For. Meteorol. 187, 14–21.

Chang, X.X., Zhao, W.Z., Zhang, Z.H., Su, Y.J., 2006. Sap flow and tree conductance of shelter-belt in arid region of China. Agric. For. Meteorol. 138, 132–141.

Chen, D.J., Xu, Z.M., Chen, R.S., 2003. Design of resources accounts: a case of integrated environmental and economic accounting. Adv. Water Sci. 14 (5), 631–637 (in Chinese with English abstract).

Cheng, X.R., Huang, M.B., Si, B.C., Shao, M.A., 2013. The differences of water balance components of *Caragana korshinkii* grown in homogeneous and layered soils. J. Arid Environ. 98, 10–19.

Cramer, V.A., Thorburn, P.J., Fraser, G.W., 1999. Transpiration and groundwater uptake from farm forest plots of Casuarina glauca and Eucalyptus camaldulensis in saline areas of southeast Queensland, Australia. Agric. Water Manag. 39, 187–204.

Dawson, T.E., Pate, J.S., 1996. Seasonal water uptake and movement in root systems of Australian phraeatophytic plants of dimorphic root morphology: a stable isotope investigation. Oecologia 107, 13–20.

Dierick, D., Holscher, D., 2009. Species-specific tree water use characteristics in reforestation stands in the Philippines. Agric. For. Meteorol. 149, 1317–1326.

Du, S., Wang, Y.L., Kume, T., Zhang, J.G., Otsuki, K., Yamanaka, N., Liu, G.B., 2011. Sapflow characteristics and climatic responses in three forest species in the semiarid Loess Plateau region of China. Agric. For. Meteorol. 151, 1–10.

Ferrante, D., Oliva, G.E., Fernández, R.J., 2014. Soil water dynamics, root systems, and plant responses in a semiarid grassland of Southern Patagonia. J. Arid Environ. 104, 52–58.

Gang, H., Xue-yong, Z., Padilla, F.M., Ha-lin, Z., 2012. Fine root dynamics and longevity of Artemisia halodendron reflect plant growth strategy in two contrasting habitats. J. Arid Environ. 79, 1–7.

Gazal, R.M., Scott, R.L., Goodrich, D.C., Williams, D.G., 2006. Controls on transpiration in a semiarid riparian cottonwood forest. Agric. For. Meteorol. 137, 56–67.

Granier, A., 1987. Evaluation of transpiration in a Douglas-fir stand by means of sap flow measurement. Tree Physiol. 3, 309–320.

Hao, X.M., Chen, Y.N., Guo, B., Ma, J.X., 2013. Hydraulic redistribution of soil water in Populus euphratica *Oliv.* in a central Asian desert riparian forest. Ecohydrology 6, 974–983.

Hodge, A., 2004. The plastic plant: root responses to heterogeneous supplies of nutrients. New Phytol. 162, 9–24.

Imada, S., Matsuo, N., Acharya, K., Yamanaka, N., 2015. Effects of salinity on fine root distribution and whole plant biomass of Tamarix ramosissima cuttings. J. Arid Environ. 114, 84–90.

Imada, S., Taniguchi, T., Acharya, K., Yamanaka, N., 2013. Vertical distribution of fine roots of Tamarix ramosissima in an arid region of southern Nevada. J. Arid Environ. 92, 46–52.

Imada, S., Yamanaka, N., Tamai, S., 2008. Water table depth affects Populus alba fine root growth and whole plant biomass. Funct. Ecol. 22, 1018–1026.

Jackson, R.B., Canadell, J., Ehleringer, J.R., Mooney, H.A., Sala, O.E., Schulze, E.D., 1996. A global analysis of root distributions for terrestrial biomes. Oecologia 108, 389–411.

Ji, X.B., Kang, E.S., Chen, R.S., Zhao, W.Z., Zhang, Z.H., Jin, B.W., 2007. A mathematical model for simulating water balances in cropped sandy soil with conventional flood irrigation applied. Agric. Water Manag. 87, 337–346.

Kizito, F., Sène, M., Dragila, M.I., Lufafa, A., Diedhiou, I., Dossa, E., Cuenca, R., Selker, J., Dick, R.P., 2007. Soil water balance of annual crop-native shrub systems in Senegal's Peanut Basin: the missing link. Agric. Water Manag. 90, 137–148.

Liu, J.X., Lin, G.J., Shen, G.L., Li, C.J., Dong, G., 1997. Preliminary investigation into the windbreak effect of farm shelter-forest network in the central section area of Hexi corridor. J. Desert Res. 17, 432–4341 (in Chinese with English abstract).

Luo, F., Qi, S.Z., Xiao, H.L., 2005. Landscape change and sandy desertification in arid areas: a case study in the Zhangye Region of Gansu Province, China. Environ. Geol. 49, 90–97.

Ma, L.H., Liu, X.L., Wang, Y.K., Wu, P.T., 2013. Effects of drip irrigation on deep root distribution, rooting depth, and soil water profile of jujube in a semiarid region. Plant Soil 373, 995–1006.

McCulley, R.L., Jobbágy, E.G., Pockman, W.T., Jackson, R.B., 2004. Nutrient uptake as a contributing explanation for deep rooting in arid and semi-arid ecosystems. Oecologia 141, 620–628.

Naithani, K.J., Ewers, B.E., Pendall, E., 2012. Sap flux-scaled transpiration and stomatal conductance response to soil and atmospheric drought in a semi-arid sagebrush ecosystem. J. Hydrol. 464–465, 176–185.

Padilla, F.M., Miranda, J.D.D., Armas, C., Pugnaire, F.I., 2015. Effects of changes in rainfall amount and pattern on root dynamics in an arid shrubland. J. Arid Environ. 114, 49–53.

Persson, H., Fircks, Y.V., Majdi, H., Nilsson, L.O., 1995. Root distribution in a Norway spruce (Picea abies (L.) Kars.) stand subjected to drought and ammonium-sulphate application. Plant Soil 168–169, 161–165.

Pinto, C.A., Nadezhdina, N., David, J.S., Kurz-Besson, C., Caldeira, M.C., Henriques, M.O., Monteiro, F.G., Pereira, J.S., David, T.S., 2013. Transpiration in Quercus suber trees under shallow water table conditions: the role of soil and groundwater. Hydrol. Process. 28, 6067–6079.

SAS Institute, 2008. SAS/STAT Users Guide. Release 6D03 edn. SAS Institute, Cary, NC.

Schenk, H.J., 2008. The shallowest possible water extraction profile: a null model for global root distributions. Vadose Zone J. 7, 1119–1124.

Schenk, H.J., Jackson, R.B., 2002. The global biogeography of roots. Ecol. Monogr. 72, 311–328.

Schenk, H.J., Jackson, R.B., 2005. Mapping the global distribution of deep roots in relation to climate and soil characteristics. Geoderma 126, 129–140.

Shen, Q., Gao, G.Y., Fu, B.J., Lü, Y.H., 2014. Soil water content variations and hydrological relations of the cropland-treebelt-desert land use pattern in an oasis-desert ecotone of the Heihe River Basin, China. Catena 123, 52–61.

Shen, Q., Gao, G.Y., Fu, B.J., Lü, Y.H., 2015. Sap flow and water use sources of shelterbelt trees in an arid inland river basin of Northwest China. Ecohydrology. http://dx.doi.org/10.1002/eco.1593.

Su, Y.Z., Wang, X.F., Yang, R., Lee, J., 2010. Effects of sandy desertified land rehabilitation on soil carbon sequestration and aggregation in an arid region in China. J. Environ. Manag. 91, 2109–2116.

Tanasescu, N., Paltineanu, C., 2004. Root distribution of apple tree under various irrigation systems within the hilly region of Romania. Int. Agrophys. 18, 175–180.

Townend, J., Reeve, M.J., Carter, A., 2001. Water release characteristic. In: Smith, K.A., Mullins, C.E. (Eds.), Soil and Environmental Analysis: Physical Methods, Revised, and Expanded, second ed. Marcel Dekker, New York, pp. 95–140.

Vincke, C., Thiry, Y., 2008. Water table is a relevant source for water uptake by a Scots pine (Pinus sylvestris L.) stand: evidences from continuous evapotranspiration and water table monitoring. Agric. For. Meteorol. 148, 419–1432.

Wilcoxa, C.S., Fergusona, J.W., Fernandezb, G.C.J., Nowaka, R.S., 2004. Fine root growth dynamics of four Mojave Desert shrubs as related to soil moisture and microsite. J. Arid Environ. 56, 129–148.

Woodall, G.S., Ward, B.H., 2002. Soil water relations, crop production and root pruning of a belt of trees. Agric. Water Manag. 53, 153–169.

Yi, J., Zhao, Y., Shao, M.A., Zhang, J.G., Cui, L.L., Si, B.C., 2014. Soil freezing and thawing processes affected by the different landscapes in the middle reaches of Heihe River Basin, Gansu, China. J. Hydrol. 519, 1328–1338.

Zeng, D.H., Jiang, F.Q., Fan, Z.P., 2002. Sustainable management for farmland shelterbelts. Chin. J. Appl. Ecol. 6, 747–749 (in Chinese with English abstract).

Zhao, W.Z., Li, Q.Y., Fang, H.Y., 2007. Effects of sand burial disturbance on seedling growth of Nitraria sphaerocarpa. Plant Soil 295, 95–102.

Zhao, W.Z., Liu, B., 2010. The response of sap flow in shrubs to rainfall pulses in the desert region of China. Agric. For. Meteorol. 150, 1297–1306.

Zhao, W.Z., Liu, B., Zhang, Z.H., 2010. Water requirements of maize in the middle Heihe River basin, China. Agric. Water Manag. 97, 215–223.

Zhou, Z.C., Shangguan, Z.P., 2007. Vertical distribution of fine roots in relation to soil factors in Pinus tabulaeformis Carr. forest of the Loess Plateau of China. Plant Soil 291, 119–129.